Verapamil as an Adjunct Therapy to Reduce tPA Toxicity in Hyperglycemic Stroke: Implication of TXNIP/NLRP3 Inflammasome

Saifudeen Ismael[1,2] · Sanaz Nasoohi[1,3] · Arum Yoo[1,2] · Golnoush Mirzahosseini[1,2] · Heba A. Ahmed[1,2] · Tauheed Ishrat[1,2,4]

Abstract

Thrombolytic therapy has remained quite challenging in hyperglycemic patients for its association with poor prognosis and increased hemorrhagic conversions. We recently showed that tissue plasminogen activator (tPA)-induced cerebrovascular damage is associated with thioredoxin-interacting protein (TXNIP) upregulation, which has an established role in the detrimental effects of hyperglycemia. In the present work, we investigated whether verapamil, an established TXNIP inhibitor, may provide protection against hyperglycemic stroke and tPA-induced blood–brain barrier (BBB) disruption. Acute hyperglycemia was induced by intraperitoneal administration of 20% glucose, 15 min prior to transient middle cerebral artery occlusion (tMCAO). Verapamil (0.15 mg/kg) or saline was intravenously infused with tPA at hyperglycemic reperfusion, 1 h post tMCAO. After 24 h of ischemia/reperfusion (I/R), mice were assessed for neurobehavioral deficits followed by sacrifice and evaluation of brain infarct volume, edema, and microbleeding. Alterations in TXNIP, inflammatory mediators, and BBB markers were further analyzed using immunoblotting or immunostaining techniques. As adjunctive therapy, verapamil significantly reduced tPA-induced BBB leakage, matrix metalloproteinase 9 (MMP-9) upregulation, and tight junction protein deregulation, which resulted in lesser hemorrhagic conversions. Importantly, verapamil strongly reversed tPA-induced TXNIP/NLRP3 (NOD-like receptor pyrin domain-containing-3) inflammasome activation and reduced infarct volume. This concurred with a remarkable decrease in high-mobility group box protein 1 (HMGB-1) and nuclear factor kappa B (NF-κB) stimulation, leading to less priming of NLRP3 inflammasome. This preclinical study supports verapamil as a safe adjuvant that may complement thrombolytic therapy by inhibiting TXNIP's detrimental role in hyperglycemic stroke.

Keywords Thioredoxin-interacting protein · Tissue plasminogen activator · Inflammasome · Verapamil · Acute hyperglycemia · Stroke

Introduction

Based on most recent reports, the absolute incidence of stroke continues to increase [1]. Acute hyperglycemia (HG) is a prevalent feature in more than 50% of admitted stroke patients [2, 3]. Based on solid clinical and preclinical evidence, acute hyperglycemia is an independent predictor of poor outcomes after stroke [4–7] and promotes neurovascular complications following thrombolytic therapy [8, 9]. A variety of adjunctive therapies have been investigated to combat neurovascular inflammation and oxidative stress [10, 11] or to improve angiogenesis and clotting kinetics [12–14] following tissue plasminogen activator (tPA) recanalization. Nevertheless, despite the profound prevalence of acute hyperglycemia in stroke patients, little has been investigated to find therapies. The high prevalence of hyperglycemia in admitted stroke patients, either for preexisting diabetes (30%) or for stress hyperglycemia (50%) [15, 16], coupled with the limitations in glucose normalization in a clinical setting [17, 18], demands investigation of new therapies in hyperglycemic patients.

Presumably, hyperglycemia and metabolic stress may recruit particular effectors to contribute to tPA-induced toxicity. High intracellular glucose concentration induces thioredoxin-interacting protein (TXNIP) [19] that is known to mediate

✉ Tauheed Ishrat
tishrat@uthsc.edu

1 Department of Anatomy and Neurobiology, College of Medicine, The University of Tennessee Health Science Center, 875 Monroe Avenue, Wittenborg Bldg, Room-231, Memphis, TN 38163, USA

2 Department of Pharmaceutical Sciences, The University of Tennessee Health Science Center, Memphis, TN 38163, USA

3 Neuroscience Research Center, Shahid Beheshti University of Medical Sciences, Tehran, Iran

4 Department of Neuroscience Institute, The University of Tennessee Health Science Center, Memphis, TN 38163, USA

hyperglycemia-induced oxidative stress [20]. Suggested as a therapeutic target in metabolic stress-induced endothelial damage [21, 22], TXNIP has a critical role in accelerating the degradation of glucose transporter-1 (GLUT-1) and deterring glucose availability to brain cells [23]. Most recently, we found that intravenous tPA is associated with TXNIP upregulation in stroked animals with acute hyperglycemia [24], which may reasonably link tPA therapy to worse outcomes in stroke [25]. Upon stimulation by oxidative stress or high glucose, TXNIP restrains thioredoxin's antioxidant activity, exacerbating the propagation of reactive oxygen species (ROS), to accelerate reperfusion injury. In the context of acute oxidative stress in ischemic–reperfusion injury, TXNIP may also stimulate the NOD-like receptor protein (NLRP3) inflammasome to assemble with apoptosis-associated speck-like (ASC) and cleaved caspase-1, which results in subsequent activation of IL-1β precursors to mature products. Based on these findings, compounds modulating TXNIP/NLRP3 inflammasome activity may work as potential adjunctive therapies to counteract tPA-associated cerebrovascular toxicity in hyperglycemic conditions.

Verapamil is a commonly prescribed and relatively safe L-type calcium channel blocker recently shown to repress TXNIP expression and subsequent inflammasome activity [26, 27]. This is in line with earlier reports on verapamil's modulatory effects on microglial cells [28]. Verapamil has long been known to provide direct protection against excessive calcium influx in ischemic/reperfusion (I/R) injury [29, 30]. However, it has not yet been investigated in hyperglycemic conditions with plausible TXNIP involvement. To address the main hypothesis, our experimental study aims to elucidate if low-dose verapamil together with tPA would ameliorate tPA-induced cerebrovascular damage in hyperglycemic stroke animals. Given that blood–brain barrier (BBB) injury is an early feature following tPA, we performed the experimental examinations and comparisons in the acute phase of a stroke at 24 h post injury [31]. Based on previous findings, the detrimental effects of the interaction between hyperglycemia and tPA on the cerebral vasculature are independent of the method of reperfusion [7]. Therefore, we utilized a clot-free transient intraluminal mouse model of stroke with tPA administration at the time of reperfusion to focus on tPA toxicity independent of the cascades following thrombolysis. We opted for the minimal effective dosage of verapamil, which was administered IV into the central compartment, with direct access to the site of action, while providing a feasible route as adjunctive therapy with tPA in the clinical setting.

Materials and Methods

Experimental Animals

All animal experiments conformed with the standard procedures approved by the Institutional Animal Care and Use Committee (IACUC) at UTHSC, Memphis, TN. The studies are reported in accordance with the ARRIVE (Animal Research: Reporting in Vivo Experiments) guidelines [32]. Adult (8–10 weeks old) male C57Bl/6 mice (Jackson Laboratory, Bar Harbor, ME, USA) were housed in standard conditions of humidity (45–50%) and temperature (21–25°C) and 12-h light/dark cycle with free access to food and water. Animals were assigned to three experimental groups: (1) MCAO + HG, (2) MCAO + HG + tPA, and (3) MCAO + HG + tPA + verapamil, with 6 animals per group (n = 6). Verapamil (Sigma, USA) was dissolved in sterile saline and administered (0.15 mg/kg, intravenously) 1 h post occlusion. The verapamil dose was determined based on previous publications [33]. Acute HG (blood glucose 300–400 mg/dl) was achieved through intraperitoneal (IP) injection of a 0.2-ml, 20% glucose solution 15 min before MCAO, as previously reported [24, 34]. Blood glucose was measured from the tail vein using a glucometer (Contour blood glucose monitoring system). The tPA (Activase, Genentech, Inc., San Francisco, CA, USA) was dissolved in sterile water and administered intravenously using a Harvard 11 Plus syringe pump (Harvard apparatus, USA). Treatment was initiated 1 h after MCAO, at a dose of 10 mg/kg with a 10% bolus and 90% infusion over 20 min. After treatment with tPA/vehicle, mice were returned to their home cages for recovery. Body temperature was maintained at 37 ± 0.5°C for the entire duration of surgery. After 24 h of MCAO, animals were deeply anesthetized with ketamine/xylazine mixture (85% and 15%, respectively) and transcardially perfused with ice-cold PBS. Animals were then decapitated and their brains collected. Serial coronal brain sections were analyzed with TTC staining and adjacent sections used for western blotting and histology. Mortality was 4 out of 22 animals, 1 animal from each of the HG MCAO and HG MCAO + tPA + Vera groups and two animals from the HG MCAO + tPA group. Animals that died were excluded from further analysis.

Induction of Focal Cerebral Ischemia

Around 22–25-g animals were subjected to transient middle cerebral artery occlusion (MCAO) using the intraluminal suture model, as described previously [35]. Briefly, animals were anesthetized using 2–5% isoflurane inhalation. A midline incision was made on the ventral surface of the neck, and the right common carotid artery was isolated and ligated. The internal carotid artery and the pterygopalatine artery were temporarily occluded using a microvascular clip. MCAO was achieved using a 6–0 silicon-coated nylon suture (Doccol, Sharon, MA), which was advanced through the internal carotid artery to block the origin of the middle cerebral artery. The mean relative cerebral blood flow observed during occlusion in mice treated with verapamil (40.84% ± 2.95%) was not significantly different from those of vehicle-treated animals (41.97% ± 3.25%). Three mice from the vehicle group and two mice from the verapamil group were excluded from the

study because of inadequate occlusion or CBF less than 40% from baseline. After 1 h, animals were re-anesthetized to remove the sutures and allow reperfusion. All the animals were maintained under anesthesia for similar durations. Body temperature was maintained at 37°C for post-surgical recovery. After reperfusion, all animals were randomized to three different groups.

Assessment of Functional Neurological Deficit Score

Neurological deficits were evaluated by a blinded investigator 24 h after I/R and just before animals were euthanized for *ex vivo* evaluations. We used the original Bederson's scale to assess for the presence/extent of deficits in our acute phase stroke studies [36]. Using the modified neurological deficit score [25], animals with no apparent deficits obtained 0; signs of impaired forelimb flexion, 1; reduced resistance to lateral push, 2; and circling, 3.

Assessment of Infarct Volume and Edema

Infarct size and edema were measured by a blinded investigator. Seven, 1-mm thick coronal sections from each brain were stained with 2% TTC solution (2,3,5-triphenyltetrazolium chloride, Sigma-Aldrich, St. Louis, MO) for 2 min at 37°C. Images of the stained sections were scanned using ImageJ analysis software (ImageJ, NIH); infarction zones were measured, and the percentage infarct volume was calculated and expressed as a percentage of the contralateral side ± SEM. Volume calculation with edema correction was performed blindly using the following formula: 100% [(infarct area/ipsilateral area) × contralateral area] [37]. Hemispheric edema was calculated as the area difference in the ischemic hemisphere compared to the contralateral hemisphere using the formula [(infarct area/ipsilateral area) × contralateral area].

Hemoglobin (Hb) Excess and Hemorrhagic Transformation (HT)

Bleeding was quantified using two different methods. (1) Cerebrovascular disruption and subsequent blood cell infiltration to the brain parenchyma were quantified using a colorimetric hemoglobin detection assay (QuantiChrom Hemoglobin Assay Kit, BioAssay Systems, Haywood, CA) to assess hemorrhagic transformation after stroke. Ipsilateral TTC-stained brain samples were separated and homogenized in a 10% glycerol Tris-buffer saline solution containing 0.5% Tween 20. Samples were analyzed for uniformly colored hemoglobin and read at 562 nm using a standard microplate reader (Synergy HT, BioTek instruments). Hemoglobin concentration was calculated according to the manufacturer's instructions and recorded in μg/dL, based on the standard, and was represented as Hb excess in the ischemic hemisphere relative to the contralateral hemisphere. (2) Hemorrhagic

occurrence rate (presence of macroscopic bleeding) was determined by visual inspection at the time of sacrifice. This was also recorded and compared between the treatment groups.

Immunoglobulin Extravasation

Extravasation of endogenous IgG was performed to accurately assess BBB permeability following stroke. Penumbral proteins (30 μg/well) were size fractionated on SDS-PAGE gels and electroblotted on a PVDF membrane. Blots were then incubated with horseradish peroxidase (HRP)-conjugated anti-mouse IgG antibody (1 : 10,000; A9044; Sigma, USA) for 1 h at room temperature and processed for visualizing the immunoreactive signal. The protein bands were quantified using ImageJ software.

Western Blotting

Whole brains were rapidly dissected into 4.0-mm coronal sections (≈0.5 and −3.5 mm from bregma) using a matrix, and peri-infarct (penumbral) regions were used for western blot analysis, as previously described [35]. Briefly, brain tissues were homogenized using a 1× radioimmunoprecipitation assay (RIPA) buffer containing protease and phosphatase inhibitor cocktails. A total of 30-μg protein was loaded into each lane and separated, followed by transfer to nitrocellulose membranes. The membranes were blocked for nonspecific binding and probed with primary antibodies against NLRP3, caspase-1, ASC (1:1000; AG-20B-0014; AG-20B-0042; AG-25B-0006, Adipogen Life Sciences), TXNIP (1:1000; NBP1-54578SS; Novus Biologicals), ZO-1, claudin 5 (1:1000; 40-2200; 33-1500; Thermo Scientific), PPARγ, HMGB1 (1:1000; SC7273; SC56698; Santa Cruz Biotechnology), claudin 5, VEGF (1:1000; 35-2500; AB-1876-1; Invitrogen), cleaved IL-1β, TNF-α, phospho-NF-κB p65 (ser536), NF-κB p65, TRX, and GLUT-1 (1:1000; 12242; 11948; 3033; 3034; 2429; 12939, Cell Signaling Technology) at 4°C overnight. Following TBS-T washes, the membranes were incubated with horseradish peroxidase (HRP)-conjugated anti-mouse IgG antibody and anti-rabbit antibody (1 : 10,000; A9044; A9169; Sigma, USA) for 1 h at room temperature. The bands were then visualized using an enhanced chemiluminescent substrate system (Thermo Fisher Scientific) and analyzed densitometrically using ImageJ 1.51J8 software. These were normalized to loading controls and expressed as fold change.

Immunofluorescence Staining

At 24 h after MCAO, mice were anesthetized with ketamine/xylazine and transcardially perfused with ice-cold PBS (30 ml) followed by 50 ml of 10% buffered formalin (Fischer Scientific). Brains were then removed and postfixed in 10% buffered formalin overnight at 4°C and then sequentially immersed in 30%

sucrose in PBS solution for 72 h. The brains were sectioned in the coronal plane at a thickness of 10 microns and blocked with serum-free protein block (X0909, DAKO), followed by incubation with primary antibodies against TXNIP (1:100; NBP1-54578SS; Novus Biologicals) and cleaved IL-1β (1:100; CST-12242, Cell Signaling Technology, USA) at 4°C overnight in a humid chamber. Sections were washed and incubated with fluorescent anti-mouse secondary antibodies (1:200; 072-04-18-03; Dylight-549, KPL) for 1 h at room temperature and mounted with ProLong™ Diamond Antifade Mountant with DAPI (Invitrogen) and viewed using a Zeiss 710 confocal laser scanning microscope. Negative controls were prepared in the same way but without the primary antibodies.

Statistical Analysis

The results were expressed as mean ± SEM. Differences among experimental groups were evaluated by Student's t-test or ANOVA followed by Tukey's post hoc test. Kruskal–Wallis test was used for nonparametric comparisons. Significance was defined by a $p < 0.05$.
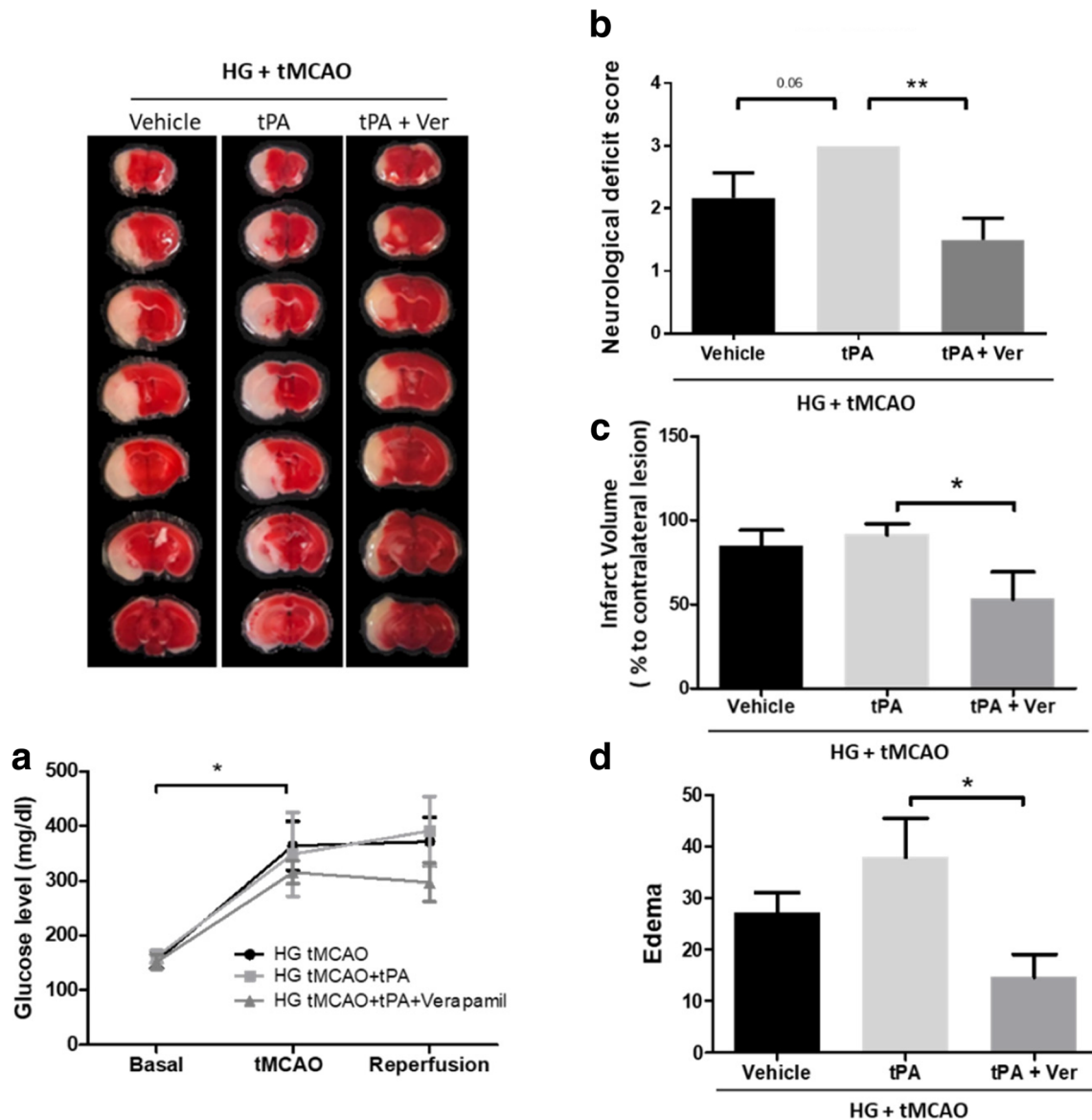

Fig. 1 Intravenous verapamil ameliorates ipsilateral edema and poor neurological outcomes in hyperglycemic stroke mice. Adult C57Bl/6 mice underwent transient middle cerebral artery occlusion (tMCAO) 15 min after a single intraperitoneal injection of 20% glucose solution. Blood glucose check confirmed the hyperglycemic (HG) states at both occlusion and reperfusion, during which, some HG tMCAO animals received intravenous tPA (10 mg/kg) with or without verapamil (Ver) (0.15 mg/kg) (a). Intravenous tPA worsened neurological function in HG tMCAO animals ($p = 0.064$). This was mitigated in verapamil-treated animals (b). Infarct volume in HG tMCAO was not affected with tPA but significantly decreased with verapamil (c). Verapamil also reduced tPA-induced ipsilateral edema, an index of cerebrovascular damage (d). All values are presented as mean ± SEM, ($n = 6$/group). *$p < 0.05$, **$p < 0.01$

Results

Verapamil Mitigates the Toxic Effects of tPA in Hyperglycemic Stroke with TXNIP Downregulation

Acute hyperglycemia (300–400 mg/dl) at the time of middle cerebral artery occlusion and reperfusion was induced by an

intraperitoneal injection of dextrose 20%. The blood glucose concentrations were not significantly affected by intravenous tissue plasminogen activator (IV-tPA) and verapamil (Fig. 1a). Based on our 3-index neurological assessment score, neurological function was moderately aggravated with IV-tPA ($p = 0.06$), as determined at 24 h after intraluminal stroke. This was discernibly prevented when verapamil was intravenously infused with
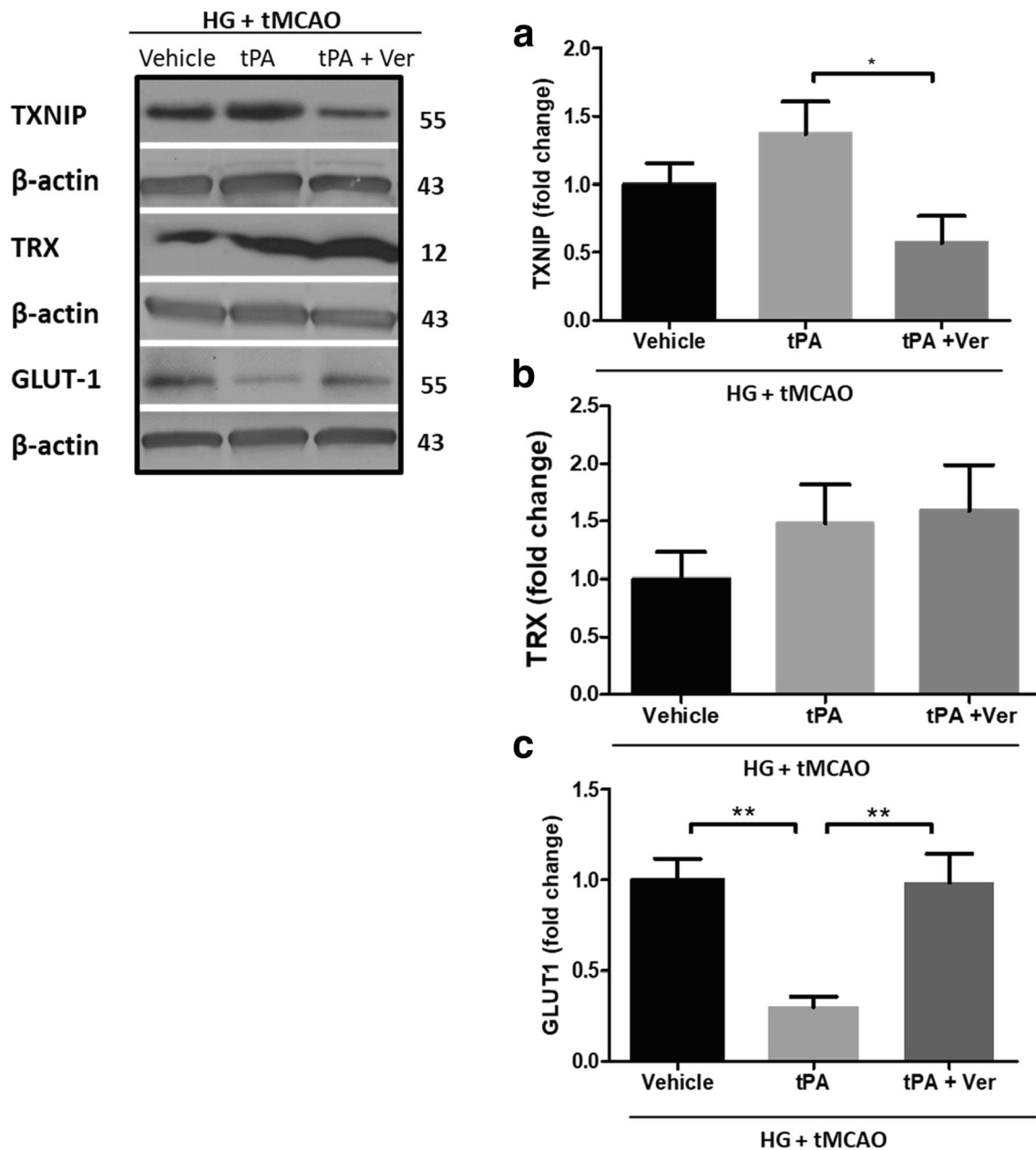

Fig. 2 TXNIP inhibition by verapamil was sufficient to reverse tPA-induced GLUT-1 downregulation. Following induction of acute hyperglycemia, adult C57Bl/6 mice were subjected to tMCAO and received intravenous (IV) tPA (10 mg/kg) with and without IV verapamil (0.15 mg/kg) at the time of reperfusion. Hyperglycemic tMCAO mice treated with tPA showed a marginal increase in brain TXNIP expression compared to untreated HG tMCAO mice. Verapamil induced a remarkable fall in TXNIP (a) but not TRX levels (b). Importantly, TXNIP alterations

with tPA and/or verapamil concurred with reciprocal changes in GLUT-1 expression, confirming a strong effect of verapamil in repression of TXNIP and consequent GLUT-1 degradation (c). All values are presented as mean ± SEM, ($n = 6$/group). *$p < 0.05$, **$p < 0.01$. Ver, verapamil; tPA, tissue plasminogen activator; HG, hyperglycemic; tMCAO, transient middle cerebral artery occlusion; TXNIP, thioredoxin-interacting protein; TRX, thioredoxin; GLUT-1, glucose transporter-1

IV-tPA (Fig. 1b). Escalation of neurological deficit scores with tPA-infusion was associated with an incremental trend in ipsilateral edema in hyperglycemic tPA + tMCAO brains with no difference in infarct volume (Fig. 1c, d), suggesting that tPA's side effects are probably linked to cerebrovascular injury [38]. A combination of intravenous verapamil with tPA at hyperglycemic reperfusion produced a remarkable attenuating effect on edema (Fig. 1d) besides producing significant neuroprotection against cerebral tissue injury (see Fig. 1c). Immunoblot analysis of brain samples further showed that verapamil profoundly reduces TXNIP expression in ipsilateral marginal ischemic tissue (Fig. 2a), with no significant effect on TRX levels (Fig. 2b). Noteworthy, TXNIP downregulation by low-dose verapamil was strong enough to lead to a meaningful rise in GLUT-1 expression in the penumbral area (Fig. 2c).

Verapamil Attenuates tPA-Induced TXNIP/NLRP3 Inflammasome Priming and Assembly in Hyperglycemic

Administration of tPA at hyperglycemic reperfusion moderately triggered NLRP3 inflammasome activation (Fig. 3), which was consistent with marginal TXNIP upregulation (see Fig. 2a). This was almost completely prevented by verapamil coadministration. Although there was no change in NLRP3 expression (Fig. 3a), verapamil reversed ASC (Fig. 3b) and caspase-1 (Fig. 3c) upregulation with tPA. Verapamil treatment further prevented tPA-induced NLRP3 inflammasome assembly and activation as determined by diminished cleaved caspase-1 (Fig. 3d) and IL-1β (Fig. 3e) production. This might be explained by verapamil's inhibitory
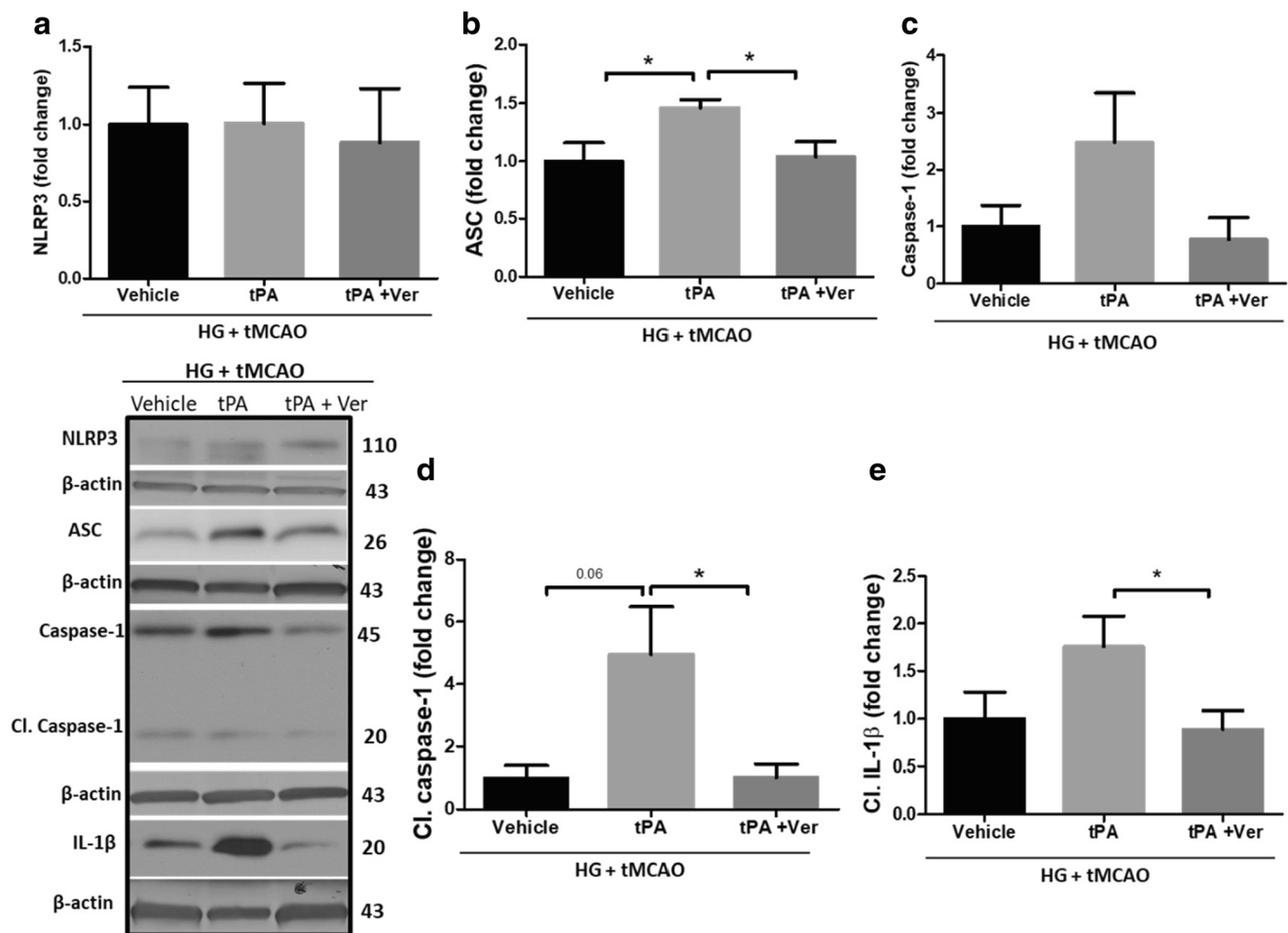

Fig. 3 tPA-induced TXNIP/NLRP3 inflammasome upregulation is blocked by verapamil coadministration. Although tPA therapy had no effect on NLRP3 component expression in hyperglycemic stroke (a), it did induce NLRP3 inflammasome priming, as indicated by ASC (b) and pro-caspase-1 upregulation (c), while also triggering inflammasome assembly, as indicated by its products, cleaved-caspase 1 (d) and IL-1β (e). Combination therapy with IV verapamil prevented NLRP3 inflammasome priming and activation. This could be explained by the remarkable TXNIP inhibition, illustrated in Figure 2. Immunostaining of the tMCAO penumbral region further confirmed discernible TXNIP/IL-1β downregulation in HG animals given IV verapamil with tPA at reperfusion (f). All values are presented as mean ± SEM, ($n = 6$/group). *$p < 0.05$. Ver, verapamil; tPA, tissue plasminogen activator; HG, hyperglycemic; tMCAO, transient middle cerebral artery occlusion; NLRP3, NOD-like receptor pyrin domain-containing-3; ASC, apoptosis-associated speck-like protein; IL-1β, interleukin 1-β
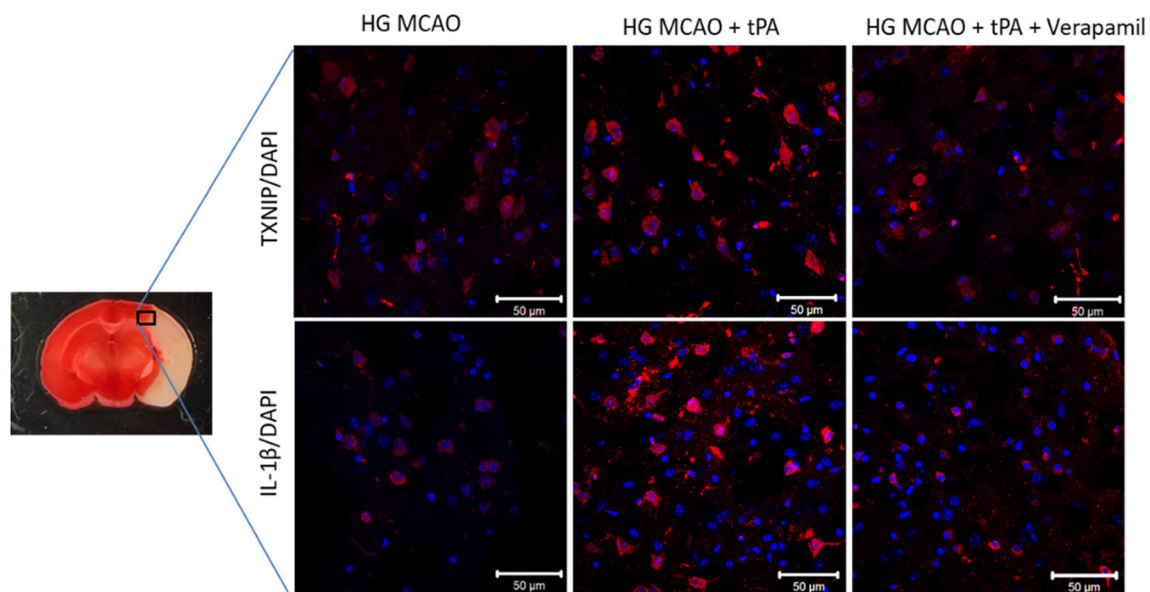
Fig. 3 continued.

effects on TXNIP, which is established to stimulate the NLRP3/IL-1β pathway. Consistently, our immunostaining examinations indicated a noticeable decrease in TXNIP and IL-1β signal in penumbral samples obtained from verapamil-treated animals (Fig. 3f). Alterations in ASC and caspase-1 resulting from tPA or verapamil indirectly reflect changes in NLRP3 inflammasome priming, where the primary constituents of inflammasome are synthesized following transcription. The parallel changes in HMGB-1/NF-κB may explain such priming effects on a transcriptional level. The priming effect is conceivably a consequence of enhanced inflammatory cytokines and immune cell recruitment concurring with NLRP3 inflammasome assembly and HMGB-1 hyperactivity. According to our immunoblotting analyses, verapamil could prevent tPA-induced HMGB-1 elevation at hyperglycemic ischemic boundaries (Fig. 4a). The slight repressive effects of verapamil on NF-κB activation ($p = 0.1$) (Fig. 4b), which lead to a strong TNF-α suppression (Fig. 4c), also demonstrate the anti-inflammatory effects of verapamil through HMGB-1/NF-κB/TNF-α, which may further explain diminished NLRP3 inflammasome priming and activity.

Adjunctive Therapy with Verapamil Blocks tPA-Induced Cerebrovascular Toxicity in Hyperglycemic Stroke

Consistent with an earlier finding [24], we discovered that IV-tPA, even when administered early, well within its golden time, may exacerbate BBB breakdown in hyperglycemic reperfusion. Gross screening of coronal sections obtained from hyperglycemic brains indicated more ipsilateral hemorrhages in those treated with tPA (Fig. 5a). However, parenchymal hemoglobin excess remained almost unchanged,

suggesting that the BBB disruption is probably more disperse in tPA-treated mice (Fig. 5b). As of our specific hypotheses, verapamil profoundly reduced hemorrhagic conversion and parenchymal hemoglobin levels in tPA-infused animals. This was precisely confirmed with immunoblotting of endogenous IgG heavy and light chains in ischemic parenchyma and indicated that verapamil strongly blocks tPA-induced BBB disruption and IgG extravasation (Fig. 5c). Matrix metalloprotease-9 (MMP-9), an established mediator of tPA-induced cerebrovascular toxicity, demonstrated a two-fold upregulation in hyperglycemic stroke animals treated with tPA (Fig. 5d). Despite significantly alleviating the effects on tPA-induced BBB breakdown, verapamil did not exert discernible effects on MMP-9 expression. However, verapamil reversed tPA-induced claudin 5 reductions (Fig. 5e). The corresponding effects of tPA on claudin 5 and zonula occludens-1 (ZO-1) (Fig. 5f) are a presumable consequence of endothelial inflammation [39] and are in agreement with earlier, in vitro reports [40], indicating MMP-9 instigates BBB breakdown through tight junctional (TJ) protein degradation.

Discussion

With its established safety profile, intra-arterial verapamil is already routinely administered in subarachnoid hemorrhage to mitigate consequent cerebral vasospasm. While existing evidence supports the benefits of verapamil in stroke, this is the first study to propose verapamil as a unique adjuvant for use with standard thrombolytic therapy in hyperglycemic stroke. Using a murine model of transient ischemic stroke, our earlier findings indicated that tPA aggravates cerebrovascular

damage in hyperglycemic reperfusion injury [24]. Here, we showed that concomitant low-dose verapamil may largely prevent tPA-associated cerebrovascular damage in hyperglycemic reperfusion injury. Our findings support the hypothesis that verapamil's protective effects are mainly due to modulating TXNIP/NLRP3 inflammasome assembly and reducing IL-1β release (Fig. 6).

Although verapamil may initiate several protective signals by blocking L-type Ca^{2+} channels, our data indicate that this compound may lead to a sharp downregulation of TXNIP in tPA-treated brains. It is known that verapamil reduces TXNIP expression, at the transcriptional level, by reducing intracellular calcium concentrations and thereby decreasing the binding of carbohydrate response element–binding protein to the promoter region of TXNIP [41]. This might further result in functional repression of TXNIP as it concurs with remarkable

GLUT-1 restoration to presumably protect against the harsh metabolic stress in hyperglycemic stroke.

Emerging evidence implies that verapamil inhibits TXNIP which appears to be critical for diabetes-associated conditions [42–44]. Indeed, verapamil-induced TXNIP modulation is believed to predict the lower incidence of type 2 diabetes [44] while conferring protection against NMDA-induced retinal neurotoxicity [45] and Alzheimer's like tau pathology [46]. In ischemic stroke, however, explanations are limited to reduced cell swelling and excitotoxicity, following Ca^{2+} influx in ischemic conditions.

Beyond its direct neuroprotective effects, verapamil is likely to protect the ischemic brain through cerebrovascular dilation and improved reperfusion [47, 48]. However consistent with the controversies, even intracerebral delivery of verapamil appears to work predominantly through direct effects at the site of
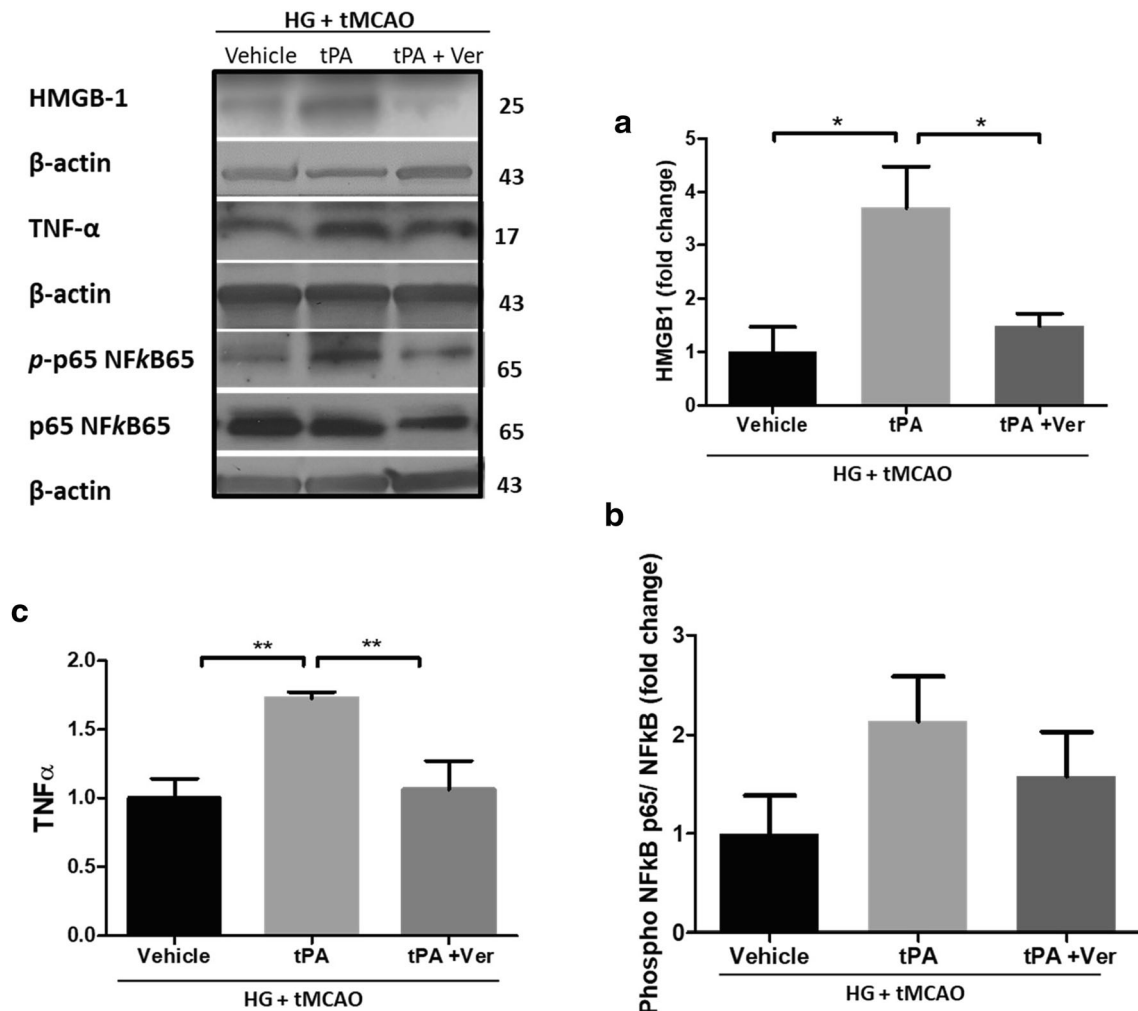

Fig. 4 Intravenous verapamil reduced tPA-associated increases in HMGB-1 and NF-κB activation in hyperglycemic stroke. Intravenous tPA (10 mg/kg) significantly upregulated HMGB-1 protein expression in HG tMCAO animals (a), leading to consequent NF-κB activation, as determined by p-p65 NF-kB/p65 NF-kB ratio (b) and further confirmed by substantial TNF-α release (c). HMGB-1/NF-κB/TNF-α activation by tPA was strongly prevented with IV verapamil (0.15 mg/kg) combination therapy. All values are presented as mean ± SEM, (n = 6/group). *p < 0.05, **p < 0.01. Ver, verapamil; tPA, tissue plasminogen activator; HG, hyperglycemic; tMCAO, transient middle cerebral artery occlusion; HMGB-1, high-mobility group box protein 1; NF-κB, nuclear factor kappa B; TNF-α, tumor necrosis factor-α
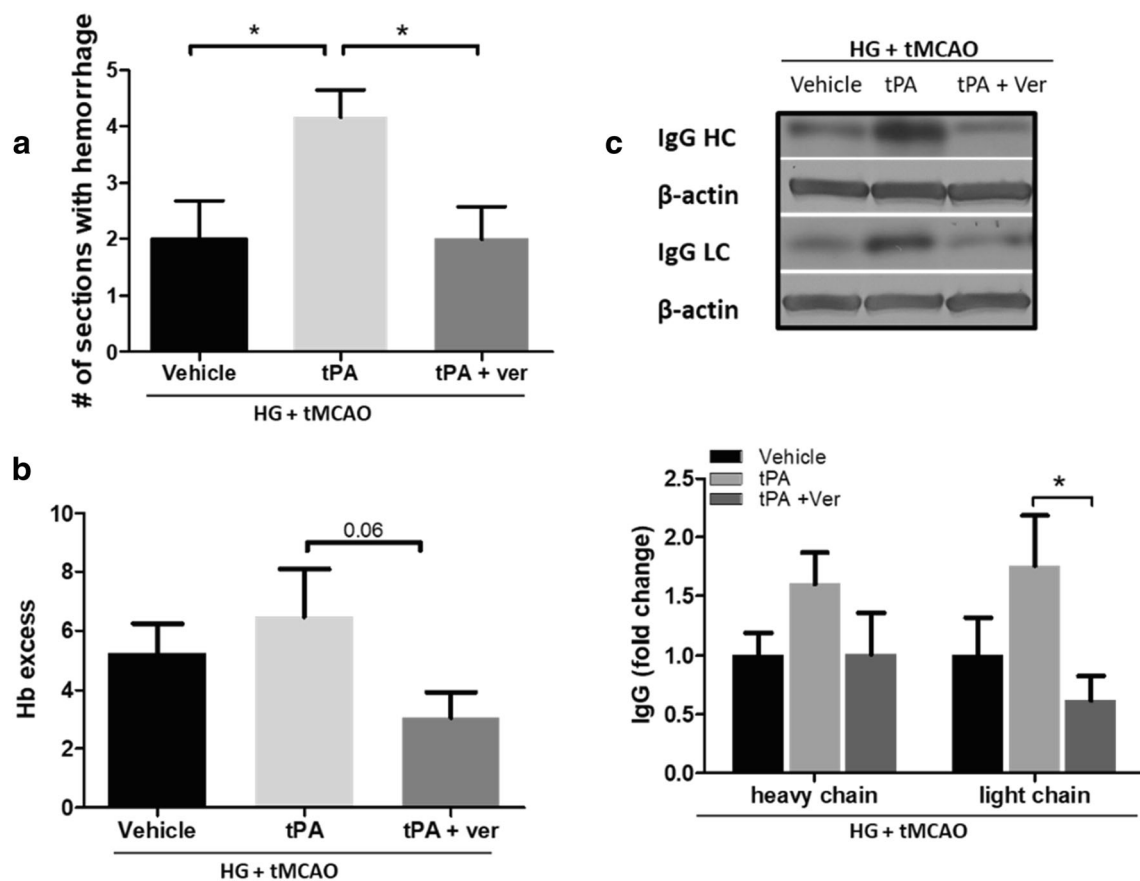
Fig. 5 BBB breakdown, following tPA therapy in hyperglycemic stroke, is attenuated by verapamil. Verapamil combination with Intravenous tPA (10 mg/kg) in HG tMCAO animals profoundly reduced ipsilateral microbleeds (a) consistent with overall Hb content in the brain parenchyma (b). Extravasation of endogenous IgG heavy and light chain also showed a discernible reduction in BBB permeability (c). In line with these alterations, verapamil combination therapy moderately repressed tPA-induced MMP-9 upregulation (d) and prevented accumulation of nonfunctional claudin 5 (e), while slightly preventing tPA-/MMP-9-induced ZO-1 degradation (f). All values are presented as mean ± SEM, (n = 6/group) *p < 0.05, **p < 0.01. Ver, verapamil; tPA, tissue plasminogen activator; HG, hyperglycemic; tMCAO, transient middle cerebral artery occlusion; MMP, matrix metalloprotease; ZO-1, zonula occludens-1

injury. In fact, the direct neuroprotective effects of low-dose intra-arterial verapamil (0.15 mg/kg) have already been demonstrated in a murine model of stroke [33]. In this study, verapamil substantially ameliorated neurological deficits, infarct volume, and apoptosis when administered at a similar dose as the one we used with filament tMCAO. In addition to its direct neuroprotective effect, verapamil produced profound BBB protection, with no effect on post-recanalization cerebral blood flow.

On the other hand, a phase I clinical trial conducted to study the safety and efficacy of intra-arterial verapamil administration post thrombectomy did not change the incidence of intracranial hemorrhage [49]. However, simulating tPA recanalization, we found a notable effect of verapamil to mitigate tPA-induced hemorrhagic transformation in HG animals. The established inhibitory effect of verapamil on TXNIP, which is critical in glucose-mediated toxicity to endothelial cells [50], may partly explain this protection.

The existing knowledge of mechanisms underlying tPA-induced BBB toxicity is greatly limited to normoglycemic conditions. Accordingly, tPA adversely affects

cerebrovascular reactivity [51] and triggers ROS generation and ultimately MMPs activation [52, 53]. Directly correlated with I/R injury [54], hyperglycemic reperfusion may presumably contribute to BBB damage following thrombolytic therapy. This is presumed to occur through NADPH oxidase-dependent ROS production consequent to glucose overflow [55], which converges on MMP-3/9 activation and BBB TJ protein deregulation [56, 57]. In our experiments, we aimed to address tPA-induced toxicity and found that tPA-induced BBB leakage in acute hyperglycemia promotes glucose-induced TXNIP/NLRP3 inflammasome signaling. The ameliorating effect we observed with verapamil, as a TXNIP inhibitor, may support the hypothesis that TXNIP is responsible for the worsened BBB leakage seen in hyperglycemic conditions. Involvement of NLRP3 inflammasome has already been supported by recent experiments in normoglycemic animals, showing that the specific NLRP3 inflammasome inhibitor (MCC950) mitigated the hemorrhagic conversion induced by delayed tPA administration [58]. IMM-H004, a derivative of coumarin, may also ameliorate tPA-induced hemorrhagic
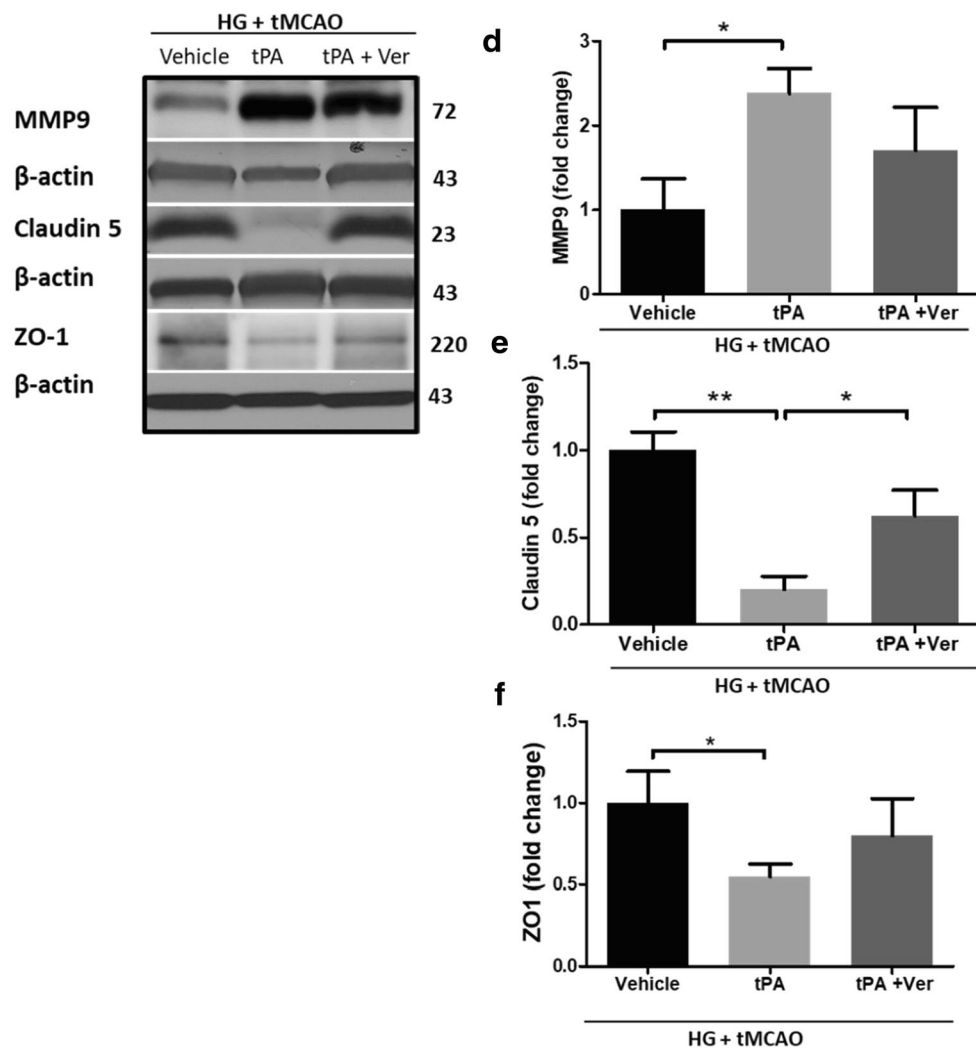
Fig. 5 continued.

transformation [59], along with NLRP3/caspase-1/IL-1β repression [60]. This is consistent with reports from our group [35] and others [40] supporting vasoprotective effects of MCC950 following intraluminal stroke. It is also important to note that verapamil not only repressed TXNIP and subsequent NLRP3 inflammasome activation (indicated by cleaved caspase-1 and IL-1β) but it also decreased the priming of NLRP3 inflammasome components (ASC and caspase-1). In line with verapamil's antimicrobial activity, this might be a consequence of HMGB-1 downregulation and activation of toll-like receptor/NF-κB signaling. HMGB1 is a nuclear non-histone DNA-binding protein and might be either actively secreted by immune cells or passively released from necrotic tissue to elicit microglial activation. HMGB-1 has been shown to closely associate with NLRP3 inflammasome activation [61, 62] to play a detrimental role in ischemic reperfusion injury [63, 64], BBB disruption [65], and tPA-induced neurovascular complications in normoglycemic rats [66].

There are some limitations to our study that are yet to be addressed in future studies. The current study is only focused on the intraluminal filament model of tMCAO with a single endpoint at 24 h. Further experimental studies are needed to evaluate the potential benefit of verapamil administrated at later time points in clinically accepted embolic model of tMCAO.

Conclusions

Thrombolytic therapy with tPA has strict limitations affecting its efficacy and safety, particularly in hyperglycemic patients. Beyond expanding tPA applicability, incorporating appropriate neuroprotective drugs to recanalization approaches may further improve their availability at the site of action. Here, we propose adjunctive therapy with low-dose verapamil, an inhibitor of TXNIP, as an efficient therapy to counteract the detrimental effects of hyperglycemia, a negative prognostic factor for hemorrhagic conversions. Our findings confirm verapamil's protective role against hyperglycemic ischemic reperfusion injury and underline the TXNIP/NLRP3
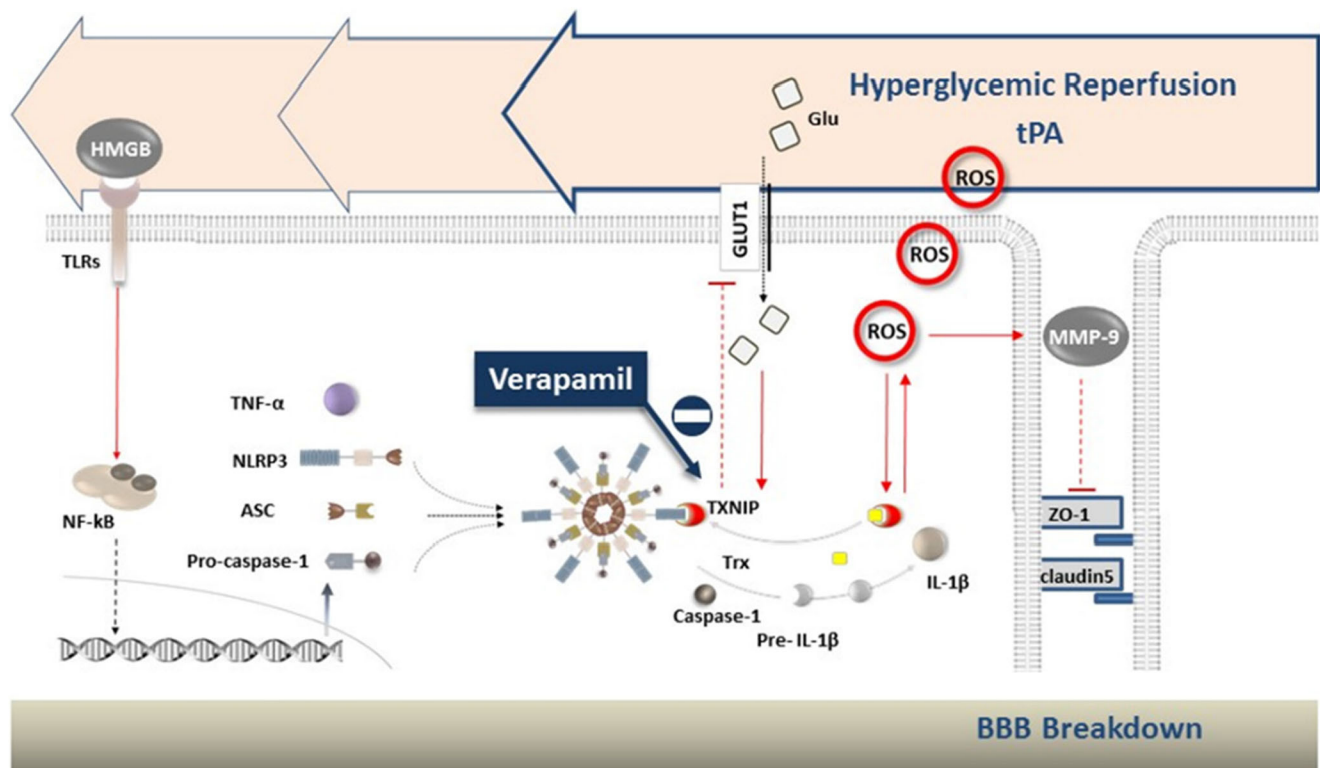
Fig. 6 Schematic diagram depicting verapamil therapeutic effects against tPA-induced toxicity in hyperglycemic stroke. Verapamil's protective role against hyperglycemic stroke, which underlines the TXNIP/NLRP3 inflammasome as a potential mediator of tPA-induced BBB breakdown. Abbreviations: GLUT-1, glucose transporter-1; HG: hyperglycemic; HMGB-1, high-mobility group box protein 1; IL-1β, interleukin 1-β; I/R, ischemic reperfusion; MMP, matrix metalloprotease; NF-κB, nuclear factor kappa B; NLRP3, NOD-like receptor pyrin domain-containing-3; TJ proteins, tight junction proteins; MCAO, transient middle cerebral artery occlusion; TNF-α, tumor necrosis factor-α; tPA, tissue plasminogen activator; TXNIP, thioredoxin-interacting protein

inflammasome as a potential mediator of tPA-induced BBB disruption in hyperglycemic conditions.

Abbreviations ASC, apoptosis-associated speck-like protein; BBB, blood–brain barrier; HG, hyperglycemic; HMGB-1, high-mobility group box protein 1; HT, hemorrhagic transformation; IL-1β, interleukin-1β; I/R, ischemic/reperfusion; MMP, matrix metalloprotease; NF-κB, nuclear factor kappa B; NLRP3, NOD-like receptor pyrin domain-containing-3; TJ, tight junction; tMCAO, transient middle cerebral artery occlusion; TNF-α, tumor necrosis factor-α; tPA, tissue plasminogen activator; TRX, thioredoxin; TXNIP, thioredoxin-interacting protein; ZO-1, zonula occludens-1

Data Availability The data generated and analyzed in this study are available from the corresponding author on reasonable request.

Declarations

All procedures related to animal studies were approved by the Institutional Animal Committee at UTHSC in full accordance with the ethical guidelines of the National Institutes of Health for the care and use of laboratory animals.

Consent to Participate   Not applicable.

Consent for Publication   Not applicable.

Conflict of Interest   The authors declare no competing interests.

References

1. Benjamin EJ, Muntner P, Bittencourt MS (2019) Heart disease and stroke statistics-2019 update: a report from the American Heart Association. Circulation 139:e56–e528

2. McCormick MT, Muir KW, Gray CS, Walters MR (2008) Management of hyperglycemia in acute stroke: how, when, and for whom? Stroke 39:2177–2185

3. Lindsberg PJ, Roine RO (2004) Hyperglycemia in acute stroke. Stroke 35:363–364

4. Skafida A, Mitrakou A, Georgiopoulos G, Alevizaki M, Spengos K, Takis K, Ntaios G, Thomadakis C et al (2018) In-hospital

dynamics of glucose, blood pressure and temperature predict outcome in patients with acute ischaemic stroke. Eur Stroke J 3:174–184

5. Hafez S, Abdelsaid M, El-Shafey S, Johnson MH, Fagan SC et al (2016) Matrix metalloprotease 3 exacerbates hemorrhagic transformation and worsens functional outcomes in hyperglycemic stroke. Stroke 47:843–851

6. Zhao L, Wang L, Lu M, Hu W, Xiu S (2019) Hyperglycemia is associated with poor in-hospital outcome in elderly patients with acute ischemic stroke. Medicine 98:e16723

7. Hafez S, Hoda MN, Guo X, Johnson MH, Fagan SC, Ergul A (2015) Comparative analysis of different methods of ischemia/reperfusion in hyperglycemic stroke outcomes: interaction with tPA. Transl Stroke Res 6:171–180

8. Bruno A, Levine S, Frankel M, Brott TG, Lin Y, Tilley BC, Lyden PD, Broderick JP et al (2002) Admission glucose level and clinical outcomes in the NINDS rt-PA stroke trial. Neurology 59:669–674

9. Tsivgoulis G, Katsanos AH, Mavridis D, Lambadiari V, Roffe C, Macleod MJ, Sevcik P, Cappellari M et al (2019) Association of baseline hyperglycemia with outcomes of patients with and without diabetes with acute ischemic stroke treated with intravenous thrombolysis: a propensity score–matched analysis from the SITS-ISTR registry. Diabetes 68:1861–1869

10. Enomoto M, Endo A, Yatsushige H, Fushimi K, Otomo Y (2019) Clinical effects of early edaravone use in acute ischemic stroke patients treated by endovascular reperfusion therapy. Stroke 50:652–658

11. Kim JS (2019) tPA helpers in the treatment of acute ischemic stroke: are they ready for clinical use? J Stroke 21:160–174

12. Zinkstok SM, Roos YB (2012) Early administration of aspirin in patients treated with alteplase for acute ischaemic stroke: a randomised controlled trial. Lancet 380:731–737

13. Berekashvili K, Soomro J, Shen L, Misra V, Chen PR, Blackburn S, Dannenbaum M, Grotta JC et al (2018) Safety and feasibility of argatroban, recombinant tissue plasminogen activator, and intra-arterial therapy in stroke (ARTSS-IA study). J Stroke Cerebrovasc Dis 27:3647–3651

14. Zhang Z, Zhang L, Yepes M, Jiang Q, Li Q, Arniego P, Coleman TA, Lawrence DA et al (2002) Adjuvant treatment with neuroserpin increases the therapeutic window for tissue-type plasminogen activator administration in a rat model of embolic stroke. Circulation 106:740–745

15. Allport L, Baird T, Butcher K, MacGregor L, Prosser J, Colman P, Davis S (2006) Frequency and temporal profile of poststroke hyperglycemia using continuous glucose monitoring. Diabetes Care 29:1839–1844

16. Furie KL, Ay H (2018) Initial evaluation and management of transient ischemic attacks and minor ischemic stroke. UpToDate, Waltham

17. Johnston KC, Bruno A, Pauls Q, Hall CE, Barrett KM, Barsan W, Fansler A, van de Bruinhorst K et al (2019) Intensive vs standard treatment of hyperglycemia and functional outcome in patients with acute ischemic stroke: the SHINE randomized clinical trial. JAMA 322:326–335

18. Bruno A, Durkalski VL, Hall CE, Juneja R, Barsan WG, Janis S, Meurer WJ, Fansler A et al (2014) The stroke hyperglycemia insulin network effort (SHINE) trial protocol: a randomized, blinded, efficacy trial of standard vs. intensive hyperglycemia management in acute stroke. Int J Stroke 9:246–251

19. Kim GS, Jung JE, Narasimhan P, Sakata H, Chan PH (2012) Induction of thioredoxin-interacting protein is mediated by oxidative stress, calcium, and glucose after brain injury in mice. Neurobiol Dis 46:440–449

20. Schulze PC, Yoshioka J, Takahashi T, He Z, King GL, Lee RT (2004) Hyperglycemia promotes oxidative stress through inhibition of thioredoxin function by thioredoxin-interacting protein. J Biol Chem 279:30369–30374

21. Bedarida T, Domingues A, Baron S, Ferreira C, Vibert F, Cottart CH, Paul JL, Escriou V et al (2018) Reduced endothelial thioredoxin-interacting protein protects arteries from damage induced by metabolic stress in vivo. FASEB J 32:3108–3118

22. Ren X, Wang N-n, Qi H, Y-y Q, C-h Z et al (2018) Up-regulation thioredoxin inhibits advanced glycation end products-induced neurodegeneration. Cell Physiol Biochem 50:1673–1686

23. Waldhart AN, Dykstra H, Peck AS, Boguslawski EA, Madaj ZB, Wen J, Veldkamp K, Hollowell M et al (2017) Phosphorylation of TXNIP by AKT mediates acute influx of glucose in response to insulin. Cell Rep 19:2005–2013

24. Ismael S, Nasoohi S, Yoo A, Ahmed HA, Ishrat T (2020) Tissue plasminogen activator promotes TXNIP-NLRP3 inflammasome activation after hyperglycemic stroke in mice. Mol Neurobiol 57:2495–2508

25. Ishrat T, Mohamed IN, Pillai B, Soliman S, Fouda AY, Ergul A, el-Remessy AB, Fagan SC (2015) Thioredoxin-interacting protein: a novel target for neuroprotection in experimental thromboembolic stroke in mice. Mol Neurobiol 51:766–778

26. Zhou F, Zhang Y, Chen J, Hu Y, Xu Y (2018) Verapamil ameliorates hepatic metaflammation by inhibiting thioredoxin-interacting protein/NLRP3 inflammasome activation. Front Endocrinol 9:640–647

27. Xu L, Lin X, Guan M, Zeng Y, Liu Y (2019) Verapamil attenuated prediabetic neuropathy in high-fat diet-fed mice through inhibiting TXNIP-mediated apoptosis and inflammation. Oxidative Med Cell Longev 2019:1–14. https://doi.org/10.1155/2019/1896041

28. Liu Y, Lo Y-C, Qian L, Crews FT, Wilson B, Chen HL, Wu HM, Chen SH et al (2011) Verapamil protects dopaminergic neuron damage through a novel anti-inflammatory mechanism by inhibition of microglial activation. Neuropharmacology 60:373–380

29. Uchida M, Takemoto Y, Nagasue N, Dhar DK, Kohno H, Nakamura T (1994) Effect of verapamil on hepatic reperfusion injury after prolonged ischemia in pigs. J Hepatol 21:217–223

30. Kimura M, Kataoka M, Kuwabara Y, Sato A, Kato T, Narita K, Okahira T, Fujii Y (1998) Beneficial effects of verapamil on intestinal ischemia and reperfusion injury: pretreatment versus postischemic treatment. Eur Surg Res 30:191–197

31. Kastrup A, Gröschel K, Ringer TM, Redecker C, Cordesmeyer R et al (2008) Early disruption of the blood–brain barrier after thrombolytic therapy predicts hemorrhage in patients with acute stroke. Stroke 39:2385–2387

32. Kilkenny C, Browne WJ, Cuthill IC, Emerson M, Altman DG (2010) Improving bioscience research reporting: the ARRIVE guidelines for reporting animal research. PLoS Biol 8:e1000412

33. Maniskas ME, Roberts JM, Aron I, Fraser JF, Bix GJ (2016) Stroke neuroprotection revisited: intra-arterial verapamil is profoundly neuroprotective in experimental acute ischemic stroke. J Cereb Blood Flow Metab 36:721–730

34. Kuroki T, Tanaka R, Shimada Y, Yamashiro K, Ueno Y, Shimura H, Urabe T, Hattori N (2016) Exendin-4 inhibits matrix metalloproteinase-9 activation and reduces infarct growth after focal cerebral ischemia in hyperglycemic mice. Stroke 47:1328–1335

35. Ismael S, Zhao L, Nasoohi S, Ishrat T (2018) Inhibition of the NLRP3-inflammasome as a potential approach for neuroprotection after stroke. Sci Rep 8(1):5971

36. Schaar KL, Brenneman MM, Savitz SI (2010) Functional assessments in the rodent stroke model. Exp Transl Stroke Med 2:1–11

37. McBride DW, Klebe D, Tang J, Zhang JH (2015) Correcting for brain swelling's effects on infarct volume calculation after middle cerebral artery occlusion in rats. Transl Stroke Res 6:323–338

38. Elgebaly MM, Ogbi S, Li W, Mezzetti EM, Prakash R, Johnson MH, Bruno A, Fagan SC et al (2011) Neurovascular injury in acute

hyperglycemia and diabetes: a comparative analysis in experimental stroke. Transl Stroke Res 2:391–398

39. Bauer AT, Bürgers HF, Rabie T, Marti HH (2010) Matrix metalloproteinase-9 mediates hypoxia-induced vascular leakage in the brain via tight junction rearrangement. J Cereb Blood Flow Metab 30:837–848

40. Li C, Wang X, Cheng F, Du X, Yan J et al (2019) Geniposide protects against hypoxia/reperfusion-induced blood-brain barrier impairment by increasing tight junction protein expression and decreasing inflammation, oxidative stress, and apoptosis in an in vitro system. Eur J Pharmacol 854:224–231

41. Xu G, Chen J, Jing G, Shalev A (2012) Preventing beta-cell loss and diabetes with calcium channel blockers. Diabetes 61:848–856

42. Poudel R, Kafle N (2017) Verapamil in diabetes. Indian J Endocrinol Metab 21:788–789

43. Perrone L, Devi T, Hosoya K, Terasaki T, Singh L (2010) Inhibition of TXNIP expression in vivo blocks early pathologies of diabetic retinopathy. Cell Death Dis 1:e65–e65

44. Thielen L, Shalev A (2018) Diabetes pathogenic mechanisms and potential new therapies based upon a novel target called TXNIP. Curr Opin Endocrinol Diabetes Obes 25:75–80

45. Al-Gayyar MM, Abdelsaid MA, Matragoon S, Pillai BA, El-Remessy AB (2011) Thioredoxin interacting protein is a novel mediator of retinal inflammation and neurotoxicity. Br J Pharmacol 164:170–180

46. Melone MAB, Dato C, Paladino S, Coppola C, Trebini C, Giordana MT, Perrone L (2018) Verapamil inhibits Ser202/Thr205 phosphorylation of Tau by blocking TXNIP/ROS/p38 MAPK pathway. Pharm Res 35(2):44–57. https://doi.org/10.1007/s11095-017-2276-2

47. Yamamoto LY, Ueda T, Shimauchi M, Diksic M (1991) Efficacy of bypass between extracerebral artery and cerebral vein with retrograde verapamil infusion into focal cerebral ischemic tissue in rats. Neurosurgery 29:719–726

48. Roy MW, Dempsey RJ, Meyer KL, Donaldson DL, Tibbs PA, Young AB (1985) Effects of verapamil and diltiazem on acute stroke in cats. J Neurosurg 63:929–936

49. Fraser JF, Maniskas M, Trout A, Lukins D, Parker L, Stafford WL, Alhajeri A, Roberts J et al (2017) Intra-arterial verapamil post-thrombectomy is feasible, safe, and neuroprotective in stroke. J Cereb Blood Flow Metab 37:3531–3543

50. Singh LP (2013) Thioredoxin interacting protein (TXNIP) and pathogenesis of diabetic retinopathy. J Clin Exp Ophthalmol 4. https://doi.org/10.4172/2155-9570.1000287

51. Hafez S, Coucha M, Bruno A, Fagan SC, Ergul A (2014) Hyperglycemia, acute ischemic stroke, and thrombolytic therapy. Transl Stroke Res 5:442–453

52. Chen H, Chen X, Luo Y, Shen J (2018) Potential molecular targets of peroxynitrite in mediating blood–brain barrier damage and haemorrhagic transformation in acute ischaemic stroke with delayed tissue plasminogen activator treatment. Free Radic Res 52:1220–1239

53. Wang X, Tsuji K, Lee S-R, Ning M, Furie KL, Buchan AM, Lo EH (2004) Mechanisms of hemorrhagic transformation after tissue plasminogen activator reperfusion therapy for ischemic stroke. Stroke 35:2726–2730

54. Won SJ, Tang XN, Suh SW, Yenari MA, Swanson RA (2011) Hyperglycemia promotes tissue plasminogen activator-induced hemorrhage by increasing superoxide production. Ann Neurol 70:583–590

55. Robbins NM, Swanson RA (2014) Opposing effects of glucose on stroke and reperfusion injury: acidosis, oxidative stress, and energy metabolism. Stroke 45:1881–1886

56. Zhang S, An Q, Wang T, Gao S, Zhou G (2018) Autophagy-and MMP-2/9-mediated reduction and redistribution of ZO-1 contribute to hyperglycemia-increased blood–brain barrier permeability during early reperfusion in stroke. Neuroscience 377:126–137

57. Desilles J-P, Syvannarath V, Ollivier V, Journé C, Delbosc S, Ducroux C, Boisseau W, Louedec L et al (2017) Exacerbation of thromboinflammation by hyperglycemia precipitates cerebral infarct growth and hemorrhagic transformation. Stroke 48:1932–1940

58. Guo Z, Yu S, Chen X, Zheng P, Hu T, Duan Z, Liu X, Liu Q et al (2018) Suppression of NLRP3 attenuates hemorrhagic transformation after delayed rtPA treatment in thromboembolic stroke rats: involvement of neutrophil recruitment. Brain Res Bull 137:229–240

59. Zuo W, Chen J, Zhang S, Tang J, Liu H, Zhang D, Chen N (2014) IMM-H004 prevents toxicity induced by delayed treatment of tPA in a rat model of focal cerebral ischemia involving PKA-and PI 3 K-dependent A kt activation. Eur J Neurosci 39:2107–2118

60. AI Q-D, chen C, Chu S-F, Zhang Z, Luo Y, et al (2019) IMM-H004 therapy for permanent focal ischemic cerebral injury via CKLF1/CCR4-mediated NLRP3 inflammasome activation. Transl Res 212:36-53

61. Chi W, Chen H, Li F, Zhu Y, Yin W, Zhuo Y (2015) HMGB1 promotes the activation of NLRP3 and caspase-8 inflammasomes via NF-κB pathway in acute glaucoma. J Neuroinflammation 12(1):137

62. Willingham SB, Allen IC, Bergstralh DT, Brickey WJ, Huang MT-H, Taxman DJ, Duncan JA, Ting JPY (2009) NLRP3 (NALP3, Cryopyrin) facilitates in vivo caspase-1 activation, necrosis, and HMGB1 release via inflammasome-dependent and-independent pathways. J Immunol 183:2008–2015

63. Liu K, Mori S, Takahashi HK, Tomono Y, Wake H, Kanke T, Sato Y, Hiraga N et al (2007) Anti-high mobility group box 1 monoclonal antibody ameliorates brain infarction induced by transient ischemia in rats. FASEB J 21:3904–3916

64. Song Y, Jun J-H, Shin E-J, Kwak Y-L, Shin J-S, Shim JK (2017) Effect of pregabalin administration upon reperfusion in a rat model of hyperglycemic stroke: mechanistic insights associated with high-mobility group box 1. PLoS One 12:e0171147

65. Zhang J, Takahashi HK, Liu K, Wake H, Liu R, Maruo T, Date I, Yoshino T et al (2011) Anti-high mobility group box-1 monoclonal antibody protects the blood–brain barrier from ischemia-induced disruption in rats. Stroke 42:1420–1428

66. Li M, Chen S, Shi X, Lyu C, Zhang Y, Tan M, Wang C, Zang N et al (2018) Cell permeable HMGB1-binding heptamer peptide ameliorates neurovascular complications associated with thrombolytic therapy in rats with transient ischemic stroke. J Neuroinflammation 15:237–250